Electronic Supplementary Information

Molten salt-mediated electrosynthesis of MoS₂ nanosheet-supported Rh nanoclusters for highly efficient electrocatalytic hydrogen evolution

Qing Yan,[ab] Yuhui Liu,[*e] Yang Zhao,[*d] Xiangqian Zhou[a] and Weiyong Yuan[*bc]

[a] *School of Biological and Chemical Engineering, NingboTech University, Ningbo 315100, P. R. China*

[b] *Ningbo Innovation Center, Zhejiang University, Ningbo, 315100, China*

[c] *College of Chemical & Biological Engineering, Zhejiang University, Hangzhou 310027, P. R. China*

[d] *College of Water Conservancy and Hydropower Engineering, Sichuan Agricultural University, Ya'an 625014, China*

[e] *East China University of Technology, Nanchang, China, 30013*

*Corresponding authors: wyyuan@zju.edu.cn (Weiyong Yuan); liuyuhui@ecut.edu.cn (Yuhui Liu); yangzhao@sicau.edu.cn (Yang Zhao)

Experimental Section

Chemicals and Materials

LiCl, KCl, $(NH_4)_6Mo_7O_{24}$, and KSCN were purchased from Tianli Chemical Reagent Co., Ltd. (Tianjin, China). $RhCl_3$ was purchased from Yului Chemical Co. Ltd (Shanghai, China). All the chemicals are of analytical grade and used without further purification. All the solutions were prepared using deionized water purified through a Milli-Q water purification system (Millipore).

Synthesis of MoS$_2$

A mixture of 35 g of LiCl and 35 g of KCl was dried at a temperature of at least 523 K under vacuum for at least 6 h for the removal of excess moisture. Subsequently, it was introduced into an alumina crucible placed inside a cylindrical quartz chamber in an electric furnace. The melting temperature is monitored using a nickel-chromium thermocouple covered with an alumina tube. Then, the anhydrous $(NH_4)_6Mo_7O_{24}$ powder and KSCN powder of analytical grade were directly introduced into the reactor to form a system composed of LiCl-KCl-$(NH_4)_6Mo_7O_{24}$-KSCN. The electrolysis was carried out at a temperature of 873 K with a current density of 1.55 A cm^{-2}. Subsequently, the black precipitate obtained was rinsed thoroughly with deionized water and anhydrous ethanol multiple times, and then subjected to vacuum drying at 333 K for 2 h.

Synthesis of MoS$_2$ NS@ Rh NC

50 mg of MoS$_2$ was dispersed in 40 mL deionized water via ultrasonication for 20 min. An appropriate volume of $RhCl_3$ solution was then added into the MoS$_2$ suspension. The reaction system was maintained at 363 K for 30 min, filtered, thoroughly washed with deionized water, and dried in vacuum at 70 °C overnight.

Characterizations

The morphologies of all the samples were examined via scanning electron microscopy (SEM, JEOL JSM-6480) and transmission electron microscopy (TEM, FEI Teccai G2 S-Twin, Philips). The crystal structures   of the samples were characterized via X-ray diffraction (XRD, Rigaku TTR III) using Cu Kα radiation (λ = 0.17889 nm) in a 2θ

range of 10-90°. The valence states of Ni and P in the sample were investigated via X-ray photoelectron spectroscopy using Al Kα radiation (XPS, Thermo ESCALAB 250).

Electrochemical Measurements

For preparation of the working electrode, 8 mg catalysts, 500 μL deionized water, 500 μL ethanol, and 32 μL Nafion solution (5 wt%) were mixed and ultrasonicated to form a suspension. 1 mg of the suspension was drop-casted on the carbon cloth and dried under an infrared lamp. The electrochemical performance of these catalysts (Ru-MoS$_2$ and controlled samples) was tested in a standard three-electrode system with linear sweep voltammetry (LSV) and chronopotentiometry (CP) on a CHI 760E electrochemical workstation. The catalyst-deposited carbon cloth was served as the working electrode, Hg/Hg$_2$Cl$_2$ electrode as the reference electrode, and a carbon rod as the counter electrode. The tests were carried out in 0.5 M H$_2$SO$_4$. Electrochemical impedance spectroscopy (EIS) measurements were performed in the frequency range of 10^5 to 0.01 Hz. The LSV curves measured for HER were *IR*-corrected. All potentials are reported versus reversible hydrogen electrode (RHE).
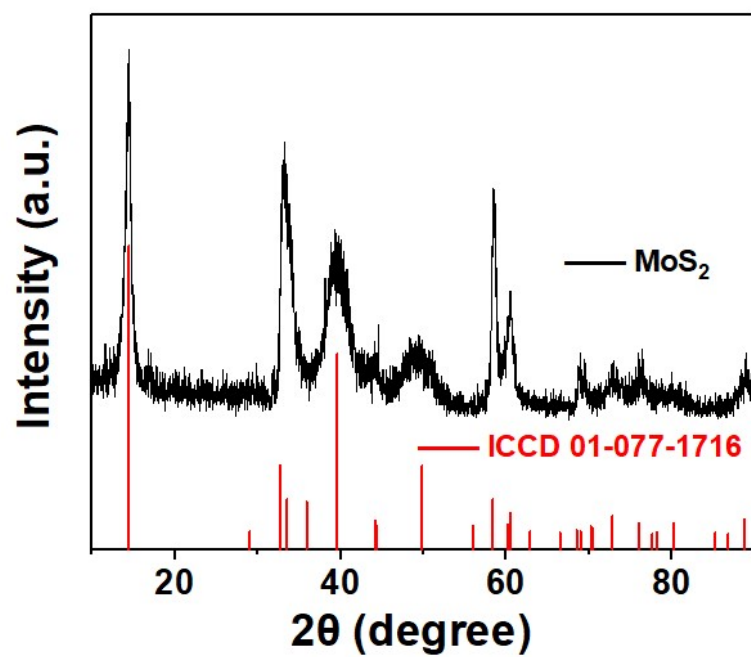
Fig. S1 XRD pattern of the MoS$_2$ sample.
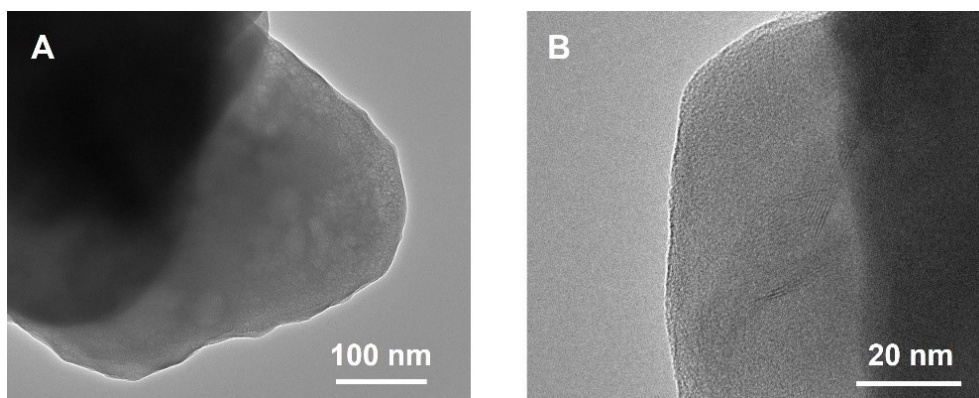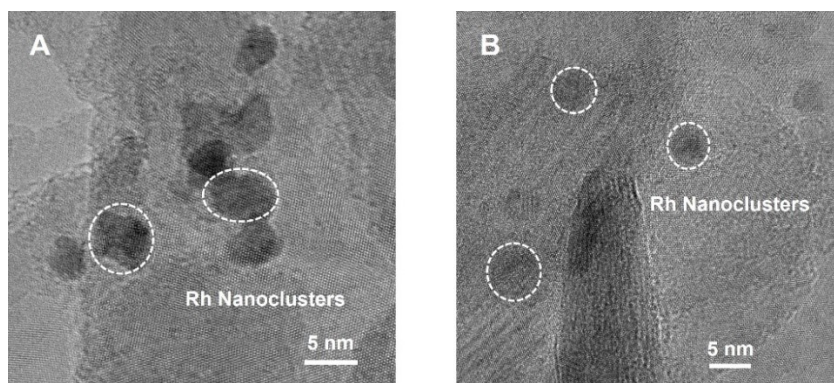

Fig. S2 The TEM image of MoS$_2$ NS.

Fig. S3 The TEM image of 7.0% MoS2 NS@Rh NC (A) and 2.8% MoS2 NS@Rh NC (B).
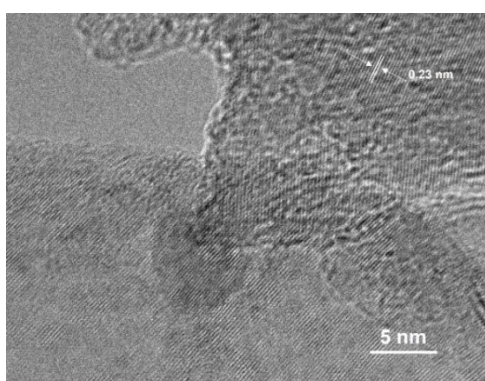

Fig. S4 The high-resolution TEM image of 3.5% MoS$_2$ NS@Rh NC.

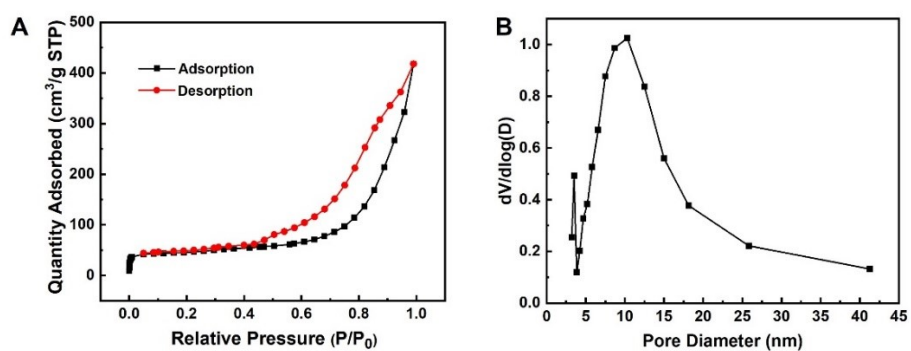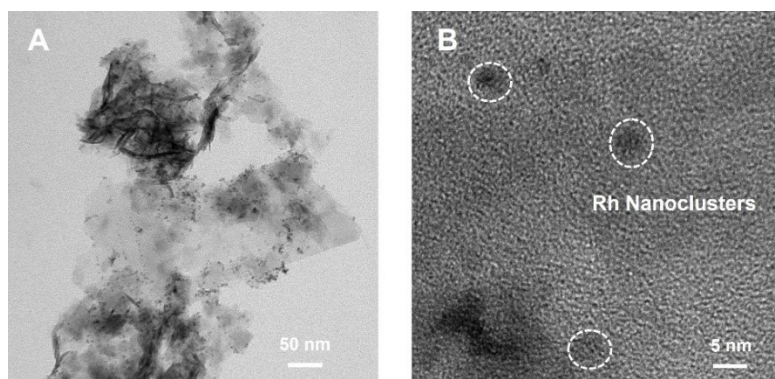**Fig. S5** The adsorption-desorption curves (A) and Pore size distribution curve (B) of 3.5% MoS$_2$ NS@Rh NC.

Fig. S6 The TEM image of 3.5% MoS$_2$ NS@Rh NC after stability testing.
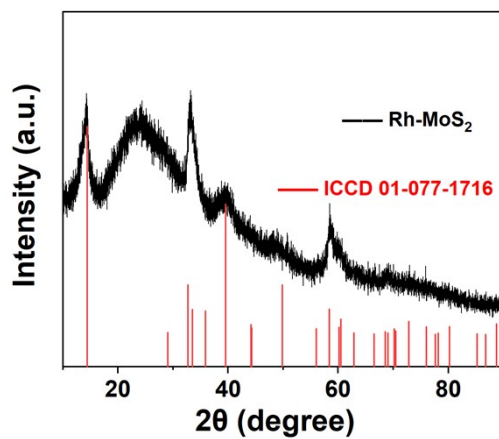

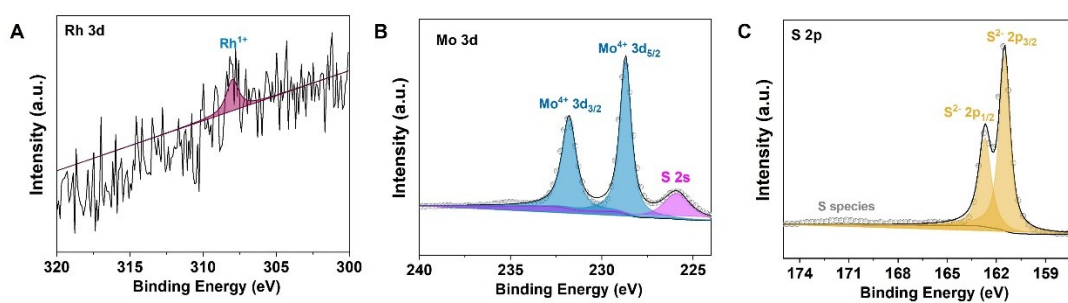**Fig. S7** The TEM image of 3.5% MoS$_2$ NS@Rh NC after stability testing.

Fig. S8 The XPS spectra of Rh 3d (A), Mo 3d (B), and S 2p (C) respectively.